Synthesis of Graphene Sheets with High Electrical Conductivity and Good Thermal Stability by Hydrogen Arc Discharge Exfoliation

Zhong-Shuai Wu, Wencai Ren,* Libo Gao, Jinping Zhao, Zongping Chen, Bilu Liu, Daiming Tang, Bing Yu, Chuanbin Jiang, and Hui-Ming Cheng*

Shenyang National Laboratory for Materials Science, Institute of Metal Research, Chinese Academy of Sciences, Shenyang 110016, P. R. China

ABSTRACT We developed a hydrogen arc discharge exfoliation method for the synthesis of graphene sheets (GSs) with excellent electrical conductivity and good thermal stability from graphite oxide (GO), in combination with solution-phase dispersion and centrifugation techniques. It was found that efficient exfoliation and considerable deoxygenation of GO, and defect elimination and healing of exfoliated graphite can be simultaneously achieved during the hydrogen arc discharge exfoliation process. The GSs obtained by hydrogen arc discharge exfoliation exhibit a high electrical conductivity of $\sim 2 \times 10^3$ S/cm and high thermal stability with oxidization resistance temperature of 601 °C, which are much better than those prepared by argon arc discharge exfoliation ($\sim 2 \times 10^2$ S/cm, 525 °C) and by conventional thermal exfoliation ($\sim$80 S/cm, 507 °C) with the same starting GO. These results demonstrate that this hydrogen arc discharge exfoliation method is a good approach for the preparation of GSs with a good quality.

KEYWORDS: graphene · synthesis · arc discharge · exfoliation · electrical conductivity · thermal stability

Graphene[1−3] has recently attracted increasing attention because of its peculiar electronic properties such as quantum Hall effect,[4] two-dimensional (2D) Dirac fermions[5] and its various promising potential applications such as composites,[6,7] transparent conductive films,[8,9] lithium-ion batteries,[10] supercapacitors,[11] organic photovoltaic cells,[12,13] electron field emitters,[14] field effect transistors,[15] and ultrasensitive sensors.[16] Several strategies are developed to produce this 2D carbon material, such as mechanical cleavage,[1] epitaxial growth on SiC[17] or metal substrates,[18] and chemical exfoliation of graphite.[19−21] Among these methods, chemical exfoliation is widely considered as a promising approach for large-scale production of graphene sheets (GSs). However, the GSs obtained by this method usually suffer from poor quality mainly due to the introduction of oxygen-containing functional groups during synthetic process, which consequently prevents their further applications, especially as electrically conductive composites and nanodevices. As a result, a post-treatment process, such as reduction of GSs by chemical method[19,21,22] or thermal annealing,[9,23] is required to remove the oxygen-containing groups. However, some structural defects such as vacancies and topological defects are simultaneously produced during the removal of functional groups. Moreover, some GSs are inevitably agglomerated during the postreduction process, resulting in an increase of the number of layers.

Recently, Hernandez *et al*. realized high-yield production of graphene free of defects or oxides by dispersion and exfoliation of graphite in organic solvents.[24] Aksay and co-workers proposed a thermal exfoliation method for the production of GSs in a large quantity, where a rapid heating process was involved to exfoliate graphite oxide (GO) by quickly moving the GO into a furnace preheated to a high temperature.[25,26] X-ray photoelectron spectroscopy (XPS) measurements indicated that the percentage of oxygen-containing functional groups was dramatically decreased, and the ratio of C/O of the final material was close to those of reduced GSs,[19] indicating that the exfoliation and partial deoxygenation of GO can be realized during this rapid heating process. However, the GSs obtained are usually a mixture of one to three layers, and suffer from relatively high oxygen-containing defects and structural defects such as vacancies and topological defects resulting from the release of carbon dioxide during deoxygenation. Recently, Wu *et al*. found that the number of layers of GSs can be tuned to some extent

*Address correspondence to cheng@imr.ac.cn, wcren@imr.ac.cn.

Received for review October 30, 2008 and accepted January 20, 2009.

Published online February 3, 2009.
10.1021/nn900020u CCC: $40.75

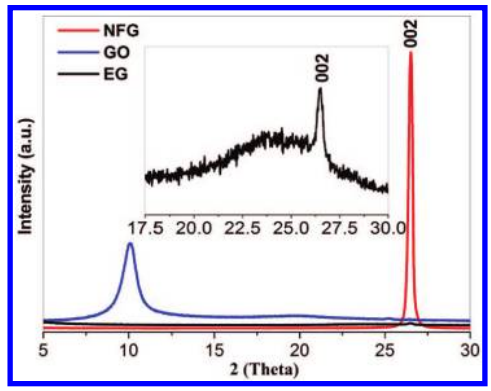

Figure 1. XRD patterns of NFG, GO, and EG. Inset: XRD pattern of EG within the range of 17.5−30°.

by using different starting graphite with different lateral size and crystallinity, and the quality of GSs can be improved by thermal treatment in H_2 atmosphere followed by exfoliation.[27] Li *et al.* prepared high-quality GSs by the thermal exfoliation−reintercalation− expansion of expandable graphite.[28] For the preparation of GSs by thermal exfoliation of GO, two properties need to be pointed out: (i) the higher the heating rate, the greater the exfoliation degrees of GO and (ii) high-temperature annealing in H_2 atmosphere is essential for deoxygenation of GO and to remove structural defects. Therefore, searching for an appropriate rapid heating method is an important way to efficiently exfoliate graphite, remove structural defects or even heal defects, and consequently obtain high-quality GSs.

The arc discharge method has been extensively used for the production of fullerenes[29] and multiwalled,[30] single-walled,[31,32] and double-walled carbon nanotubes (CNTs).[33,34] Compared to chemical vapor deposition method, CNTs synthesized by arc discharge method, especially in the presence of hydrogen, have merits of good crystallinity and high thermal stability due to an *in situ* defect-healing effect of the high plasma temperature and the etching effect of H_2 on amorphous carbon.[33,34] Moreover, the temperature can be instantaneously increased to more than 2000 °C during arc discharge process. Therefore, it is reasonable to expect that hydrogen arc discharge heating can be used for efficient exfoliation and considerable deoxygenation of GO, and defect elimination and healing of the resultant exfoliated graphite (EG). In this paper, we demonstrated hydrogen arc discharge as a rapid heating method to produce GSs with a good quality from GO, combining with solution-phase dispersion and centrifugation techniques. The GSs obtained exhibit a high electrical conductivity of $\sim 2 \times 10^3$ S/cm and high thermal stability with an oxidization resistance temperature of 601 °C, which are much better than those prepared by argon arc discharge exfoliation ($\sim 2 \times 10^2$ S/cm, 525 °C) and by conventional thermal exfoliation (~80 S/cm, 507 °C).

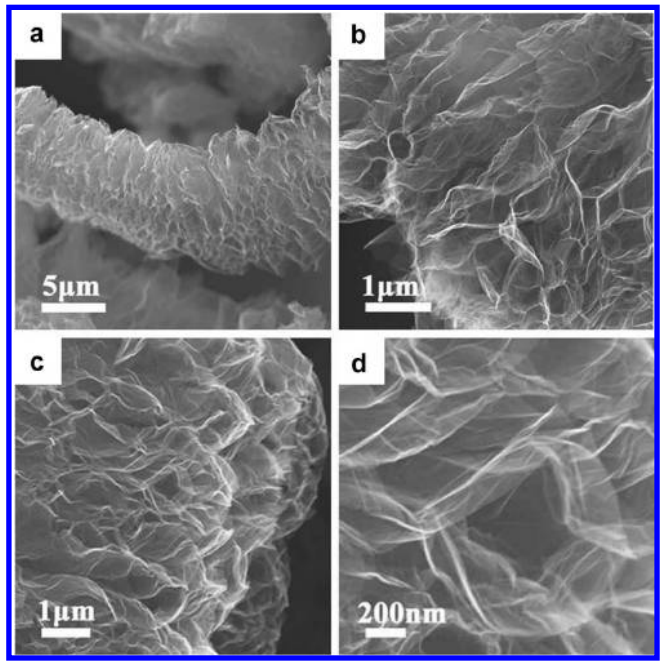

Figure 2. SEM images of hydrogen arc discharge-exfoliated EG: (a) EG with a transparent wormlike morphology, (b) top view and (c) side view of the EG; (d) magnification of a part of the EG in panel c.

RESULTS AND DISCUSSION

Figure 1 shows the X-ray diffraction (XRD) patterns of the starting graphite (natural flake graphite, NFG), GO obtained by Hummers method,[27,35] and H_2 arc discharge-exfoliated EG. It can be found that the interlayer spacing was increased from 3.35 Å for NFG to 8.3 Å for GO without (002) diffraction peak of graphite, indicating that the graphite was efficiently oxidized.[26] Because the temperature can instantaneously reach more than 2000 °C in less than 20 s during arc discharge process, the decomposition rate of the oxygen-containing groups of GO will exceed the diffusion rate of the evolved gases during this rapid heating process, thus yielding pressure that exceeds the van der Waals force holding the graphene sheets together in GO. The obtained EG (Figure 1) shows a weak (002) peak and a broader peak at 20−30°, which illustrates that the stacking of EG is substantially disordered.[36] This can be confirmed by scanning electron microscopy (SEM) observations. Low-magnification SEM image (Figure 2a) of EG shows that it has a transparent accordion- or wormlike structure. Top-view SEM (Figure 2b) and side-view SEM (Figure 2c) images reveal that most of the GO were efficiently exfoliated to form separated ultrathin sheets (Figure 2d). However, we should note that the specific surface area (570 m^2/g) of the EG (Figure 3) is much smaller than the theoretical specific surface area of single-layer GSs (2620 m^2/g), indicating that some of the GO were not well exfoliated or some of the individual sheets in the EG were agglomerated and overlapped. Therefore, both sonication and centrifugation processes are required to obtain single-layer GSs.

After GO was exfoliated by hydrogen arc discharge, the EG can be easily conversed to GSs through sonica-

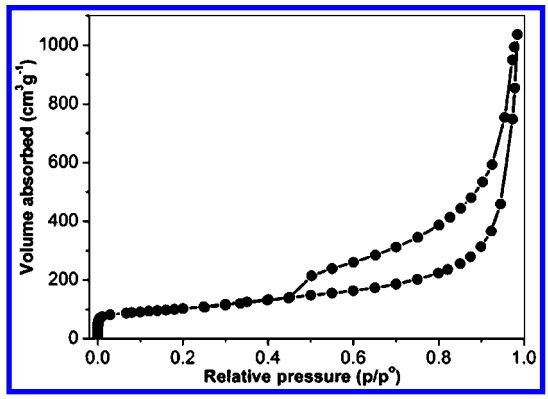

Figure 3. Nitrogen adsorption and desorption isotherms of the hydrogen arc discharge-exfoliated EG.

tion and centrifugation, and a homogeneous GS-containing supernatant was obtained. Transmission electron microscopy (TEM) and atomic force microscopy (AFM) were used to characterize the structure of the as-prepared GSs. Low-magnification TEM (Figure 4a) observation shows that the hydrogen arc discharge exfoliated GS looks like a transparent thin sheet with a few folds within its plane. This is quite different from the GSs prepared by conventional thermal exfoliation,[10,26,37] which generally looks like a wrinkled or crumpled thin paperlike structure with many folds within the plane in low-magnification TEM image. This flat structure is also demonstrated by AFM (Figure 4b and 4c), indicating the higher quality of GSs than those prepared by conventional thermal exfoliation. On the basis of AFM measurements on hundreds of GSs, we found that ~80% GSs have a topographic height of 0.9−1.1 nm as shown in Figure 4b,c, which are considered to correspond to single-layer GSs.[19,25,26,28] This can be further confirmed by the 2D band of GSs located at ~2644 cm^{-1} (Figure 4d), which is consistent with that reported for the single-layer GSs prepared by micromechanical cleavage[38,39] and chemical exfoliation and followed reduction of GO.[9] On the basis of the mass of the single-layer GSs in the supernatant and the starting graphite, it can be estimated that our process can produce single-layer GSs at a yield of ~18 wt % after first dispersion and centrifugation. We should point out that the yield of single-layer GSs can be further increased to ~50 wt % of the starting graphite with sediment recycling for several times.

To further evaluate the quality of H_2 arc discharge-exfoliated GSs, XPS measurements were employed to analyze the content of residual oxygen-containing functional groups in the sheets. For comparison, the starting graphite (*i.e.*, NFG) and the GSs obtained by conventional thermal exfoliation and argon arc discharge exfoliation were also measured. Figure 5a shows that the C1s peak of H_2 arc discharge-exfoliated GSs is similar to that of starting graphite, without significant signals of C−O species of GO. Elemental analysis based on XPS measurements further reveals that H_2 arc discharge-exfoliated GSs have a C/O molar ratio of 15−18, which is higher than that of Ar arc discharge-exfoliated GSs (~12), conventional thermally exfoliated GSs (~9.4), conventional thermally exfoliated GSs followed by H_2 reduction (~14.9),[27] and chemically reduced GSs (~10) by hydrazine,[19] and comparable to that reported for conventional thermally exfoliated GSs (10−20).[25,40] We also measured the Fourier transform infrared (FTIR) spectra of the GSs prepared by different methods and the results are shown in Figure 5b. It can be found that much weak signal for the C═O stretching vibrations at 1730 cm^{-1} was observed for GSs prepared by hydrogen arc discharge exfoliation compared to those prepared by Ar arc discharge exfoliation and conventional thermal exfoliation, which is similar to that of the GSs prepared by the thermal exfoliation-reintercalation-expansion method.[28] These results suggest that H_2 arc discharge exfoliation is a more effective method to remove oxygen-containing groups than the commonly used thermal exfoliation and postreduction.

Raman spectroscopy provides a powerful tool to determine the quality of carbon materials. Therefore, we performed Raman measurements on the GSs obtained by different heating methods. We directly spin-coated the graphene supernatants onto a SiO_2/Si wafer for Raman measurements, instead of graphene powders, to weaken the contribution of edges to the D-band intensity. Figure 6 compares the 632.8 nm Raman spectra of H_2 arc discharge-, Ar arc discharge-, and conventional thermally exfoliated GSs. All the Raman spectra of the as-prepared GSs displays two prominent peaks at

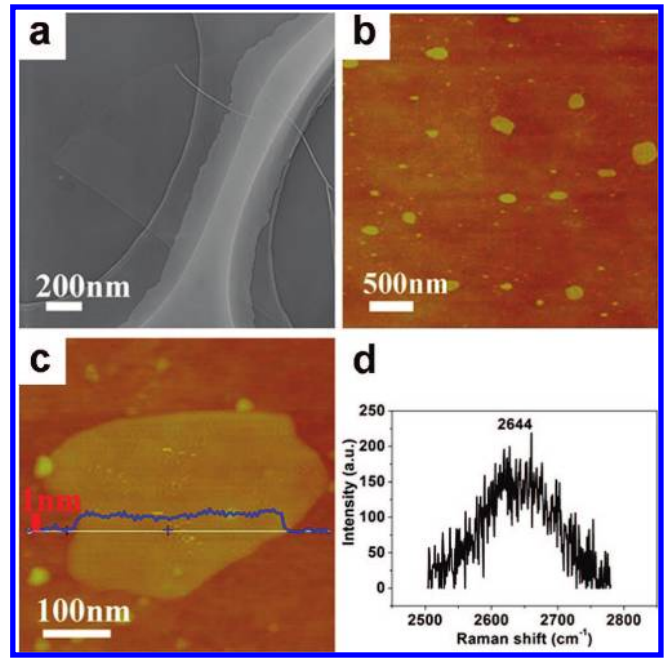

Figure 4. Structural characterization of the hydrogen arc discharge-exfoliated GSs. (a) Typical low-magnification TEM image of GSs. (b, c) Tapping-mode AFM images of GSs obtained by spin-coating the supernatant onto a 300 nm SiO_2/Si wafer. Inset of panel c: The corresponding height profile. (d) Typical 2D-band profile of single-layer GSs, taken with a laser energy of 1.96 eV.

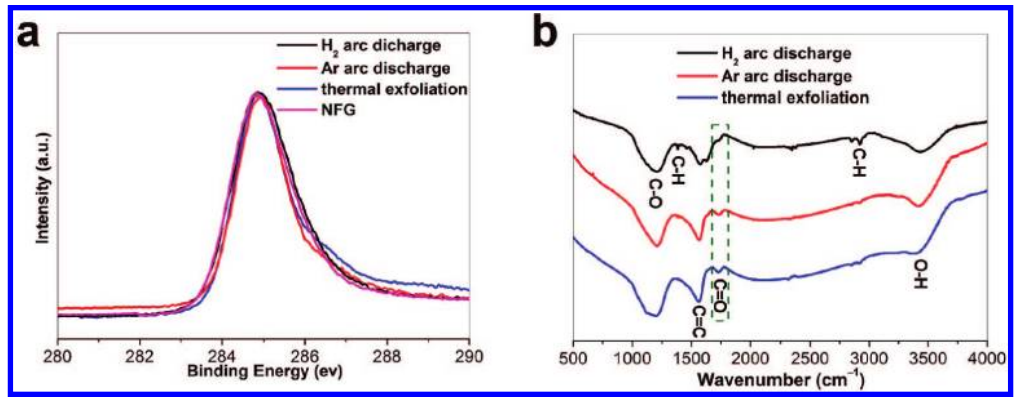

Figure 5. (a) XPS of NFG, H_2 arc discharge-, Ar arc discharge-, and conventional thermally exfoliated GSs. (b) FTIR spectra of H_2 arc discharge-, Ar arc discharge-, and conventional thermally exfoliated GSs. The dot square frame indicates the signals of C═O stretching vibrations.

~1330 and ~1590 cm^{-1}, which correspond to the well-documented D band and G band, respectively.[40] It is well-known that G band corresponds to the first-order scattering of the E_{2g} mode observed for sp^2 carbon domains, and the pronounced D band is disordered band associated with structural defects, amorphous carbon or edges that can break the symmetry and selection rule.[39] A universal observation is that higher disorder in graphite leads to a broader G band, as well as to a broad D band of higher relative intensity compared to that of the G band. Therefore, the intensity ratio of D band to G band (I_D/I_G) is usually used as a measure of the disorder.[39,41,42] For example, Kudin *et al*. systematically investigated the Raman spectra of GO and GSs prepared by thermal expansion/exfoliation,[40] and they found that the I_D/I_G of GSs was decreased compared to that of GO, attributed to a graphitic "self-healing" similar to what was observed for the intensity decrease of the D band in heat-treated graphite.[42,43] Here we also use it as an indicator of the quality of the obtained GSs. The I_D/I_G of Ar arc discharge-exfoliated GSs shows a noticeable decrease compared to that of conventional thermally exfoliated GSs. However, it is worth noting that a dramatic decrease of the I_D/I_G was observed for H_2 arc discharge-exfoliated GSs, indicating a much better quality than those of Ar arc discharge and conventional thermally exfoliated ones. We should note that our GSs (with a size normally <500 nm) are much smaller than the used laser spot (typically ~1 μm^2), and consequently graphene edges made considerable contribution to the D band intensity. Therefore, the quality of GSs prepared by hydrogen arc discharge exfoliation should be underestimated by the I_D/I_G.

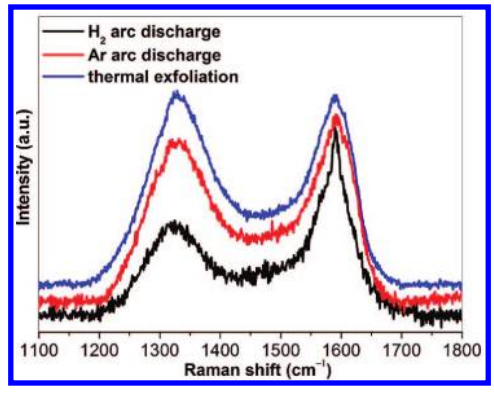

Figure 6. G-band intensity normalized Raman spectra of H_2 arc discharge-, Ar arc discharge-, and conventional thermally exfoliated GSs, taken with a laser energy of 1.96 eV.

It is generally accepted that the thermal stability of a carbon material toward high-temperature air oxidation can be increased with improving its quality. Therefore, we have also performed thermogravimetry/derivative thermogravimetry (TG/DTG) measurements to evaluate the quality of the GSs obtained by different heating methods. Figure 7 shows the TG/DTG curves of H_2 arc discharge-, Ar arc discharge-, and conventional thermally exfoliated GSs. It can be found that the arc discharge-exfoliated GSs are more stable to high-temperature air oxidation than those obtained by conventional thermal exfoliation. In the case of arc discharge exfoliation, the oxidation resistance temperature of GSs is remarkably increased when a portion of H_2 was added into the reaction system instead of pure argon, as shown in Figure 7a. Compared with those obtained by conventional thermal exfoliation (507 °C), the oxidation resistance temperature of Ar (525 °C) and H_2 (601 °C) arc discharge-exfoliated GSs were increased 18 and 94 °C, respectively, based on the T_{max} (temperature corresponding to the highest combustion rate) of DTG in Figure 7b. This further proves the good quality of the H_2 arc discharge-exfoliated GSs, and suggests that both arc discharge heating and H_2 play important roles in improving the quality of GSs. Normally, the conventional thermally exfoliated GSs contain some oxygen-containing groups at their edges and on their basal planes due to the oxidation process even though most of them can be removed during thermal expansion (typically <1100 °C). Moreover, some vacancies and topological defects can be simultaneously produced on the sheets because of the release of carbon dioxide during the thermal expansion/exfoliation process in Ar atmosphere. These defect sites lead to a de-

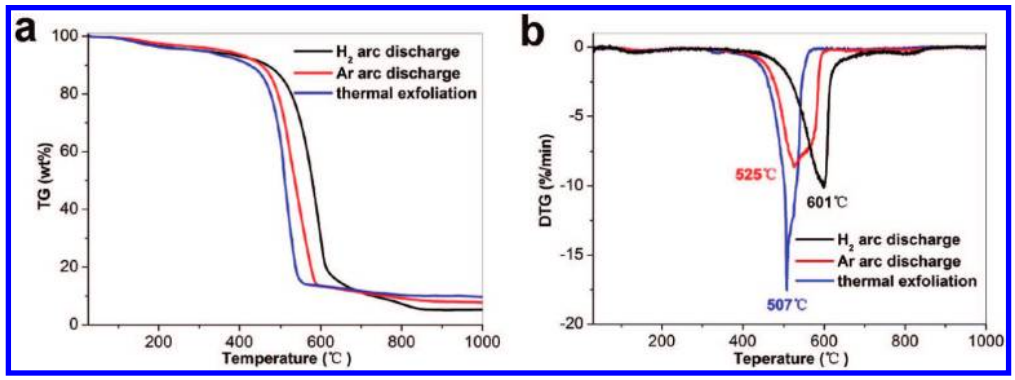

Figure 7. (a) TG and (b) DTG curves of H_2 arc discharge-, Ar arc discharge-, and conventional thermally exfoliated GSs.

crease in the thermal stability of these materials at elevated temperature. When H_2 is added to the Ar atmosphere, the oxygen-containing groups tend to be removed in the form of H_2O instead of CO_2 in some extent, avoiding the production of vacancies and topological defects because of less loss of carbon atoms. More importantly, high plasma temperature (>2000 °C) in arc discharge exfoliation can facilitate the removal of functional groups and heal the defects.[33,34,42−47] Therefore, H_2 arc discharge-exfoliated GSs display higher quality and thermal stability toward high-temperature oxidation than those obtained by Ar arc discharge and conventional thermal exfoliation.

To study the effect of rapid heating mode and atmosphere on the electrical conductivity of GSs, we investigated the current−voltage (*I*−*V*) characteristics of individual H_2 arc discharge-, Ar arc discharge-, and conventional thermally exfoliated GSs, using a Nanofactory TEM-scanning tunneling microscopy (STM) sample holder inside a TEM, as illustrated in Figure 8a. It is clearly seen from Figure 8b that the current through H_2 arc discharge-exfoliated GS is much larger than that through Ar arc discharge-exfoliated and conventional thermally exfoliated GS under the same applied voltages, indicating a pronounced decrease of the electrical resistance. We calculated the electrical conductivity of GS on the basis of the most commonly used thermionic emission model for Schottky contacts,[48] mainly considering the nonlinear symmetric *I*−*V* characteristics and the contact resistance contributions between the electrodes and GSs. The electrical conductivity of H_2 arc discharge-exfoliated GSs (~2×10^3 S/cm) is higher by a factor of 10 than that of Ar arc discharge-exfoliated GSs (~2×10^2 S/cm), and both of them are much larger than that (~80 S/cm) of conventional thermally exfoliated GSs. Considering the above structural comparison, we reason that the improvement of electrical conductivity of the H_2 arc discharge-exfoliated GSs is attributed to the *in situ* defect elimination and healing of EG during the exfoliation. Several groups have also developed various methods to reduce the as-prepared GSs and to improve their electrical conductivity.[9,19,21−23,27] For example, Gomez-Navarro *et al*. found that the electrical conductivity of the reduced GO by hydrazine and hydrogen plasma is increased 10^3 times than the pristine GO.[22] However, this improved conductivity is still smaller with a factor of 10^3−10^4 than that of our H_2 arc discharge−exfoliated GSs. This indicates that the electrical properties of graphene can be tuned by different rapid heating methods and our proposed H_2 arc discharge exfoliation method is a better way to improve the electrical conductivity of GSs, which will be very helpful for their electrical transport-related applications such as nanoelectronic devices, conductive composites, transparent conductive films, and electrode materials for lithium-ion battery and supercapacitor.

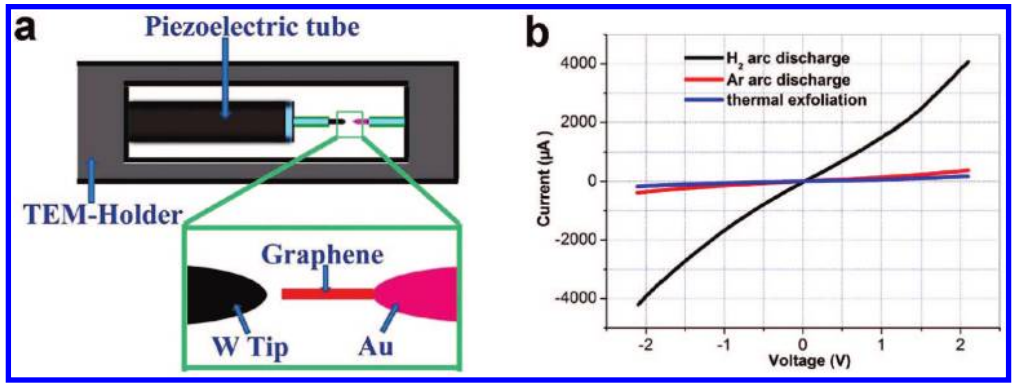

Figure 8. Electrical conductivity measurements of the GSs prepared by different heating methods: (a) schematic of the TEM-STM sample holder; (b) typical *I*-*V* curves of H_2 arc discharge-, Ar arc discharge-, and conventional thermally exfoliated GSs.

CONCLUSIONS

We have developed a hydrogen arc discharge exfoliation technique for the synthesis of GSs with a good quality from GO, combining with solution-phase dispersion and centrifugation techniques. It was found that the GSs obtained by hydrogen arc discharge exfoliation have a good electrical conductivity of $\sim 2 \times 10^3$ S/cm and high thermal stability with oxidization resistance temperature of 601 °C, which are much better than those prepared by argon arc discharge exfoliation ($\sim 2 \times 10^2$ S/cm, 525 °C) and by conventional thermal exfoliation ($\sim$80 S/cm, 507 °C). On the basis of the structural characterization and exfoliation process analysis, we suggest that the high plasma temperature and reducing H_2 during hydrogen arc discharge exfoliation play important roles in efficient exfoliation and considerable deoxygenation of GO, and defect elimination and healing of EG, which are responsible for the production of high-quality GSs. Our findings also indicate that the electrical properties of GSs can be tuned by different heating modes. The preparation of the highly conductive GSs opens up a possibility to a wide range of technological applications including graphene-based nanoelectronics, transparent conductive films, conductive composites, lithium ion batteries, and supercapacitors.

METHODS

The preparation of H_2 arc discharge-exfoliated GSs mainly involves three key steps: oxidation of graphite, subsequent exfoliation of the resulting GO by hydrogen arc discharge, and dispersion of EG to obtain GSs by ultrasonication. NFG (500 mesh) as starting graphite was first oxidized by the Hummers method to prepare GO, as we previously reported elsewhere.[27] In a typical experiment, 1 g of graphite, 0.5 g of $NaNO_3$ and 23 mL of concentrated H_2SO_4 were mixed and stirred at 0 °C. Then 3 g of $KMnO_4$ was added slowly to the above solution with stirring and cooling. After this, the suspended solution was stirred continuously for 12 h, and 46 mL of distilled water was added slowly to the suspension for 15 min. Subsequently, the suspension was added by 140 mL of warm water (40$\sim$50 °C) and 10 mL of H_2O_2 (30%). Finally, the resulting suspension was filtered, washed with deionized water, and dried in a vacuum oven at 60 °C for 24 h to obtain GO. After the as-prepared GO was fully dried in vacuum, it was then rapidly heated by arc discharge in a mixed buffer gas of H_2 ($\leq$10 kPa pressure) and argon (90 kPa pressure) to obtain EG. The cathode is a graphite rod (10 mm in diameter and 150 mm in length), and the anode is a rotatable graphite cylinder with eight holes (20 mm in diameter and 10 mm in depth each) used to load GO. The distance of two electrodes was maintained about 2 mm, and high-temperature discharge between the two electrodes was generated by a direct current mode ranging from 100 to 150 A. The resulting EG (10 mg) was dispersed in 10 mL of *N*-methylpyrolidone (NMP) for 2 h by sonication to form a homogeneous suspension. Then, the suspension was centrifuged at 15000 rpm for 5 min to remove thick GSs and nonexfoliated graphite, and to retain thin GSs in the supernatant. For comparison, Ar arc discharge-exfoliated GSs and conventional thermally exfoliated GSs were also prepared from the same GO by argon arc discharge and by quickly moving the GO into a preheated tube furnace (1050 °C) in argon atmosphere, respectively, combining with the same sonication and centrifugation processes as those for the preparation of hydrogen arc discharge-exfoliated GSs.

XRD (D/max 2400 with Cu kα radiation), XPS (Escalab 250, Al kα), IR (Nicolet 605XB FTIR spectrometer, KBr background), Raman spectroscopy (Jobin Yvon LabRam HR800, excited by 632.8 nm laser), TG/DTG (Netzsch-STA 449C, measured from 30 to 1000 °C at a heating rate of 10 °C/min in air), nitrogen cryosorption (Micromeritics, ASAP2010M), SEM (LEO, Supra 35, 15 kV), TEM (JEOL JEM 2010, 200 kV), and AFM (Veeco MultiMode/NanoScope IIIa) were used to characterize the GO, EG, and GSs. The TEM samples were prepared by drying a droplet of the graphene suspension onto a Cu grid with a holey carbon film, and the AFM samples were prepared by spin coating the graphene supernatant onto a 300 nm SiO_2/Si substrate. The electrical conductivity of the GSs obtained was measured inside a JEOL JEM-2010 TEM equipped with a Nanofactory TEM-STM system (ST1000), which integrates a fully functional STM into a TEM. The STM probe was controlled by a piezo-manipulator that can approach individual nanostructures inside the TEM. The obtained supernatant after centrifugation treatment was filtered and then dried in a vacuum oven at 60 °C for 24 h. The resulting GS powders were attached to an Au electrode, and the tungsten STM tip was controlled precisely in the TEM to connect the selected GS to measure its electrical conductivity. The applied voltages were in the range of $-2.5-2.5$ V.

Acknowledgment. This work was supported by National Science Foundation of China (No. 50872136 and No. 90606008), MOST of China (No. 2006CB932703), Chinese Academy of Sciences (No. KJCX2-YW-M01), and the Knowledge Innovation Program of CAS.

REFERENCES AND NOTES

1. Novoselov, K. S.; Geim, A. K.; Morozov, S. V.; Jiang, D.; Zhang, Y.; Dubonos, S. V.; Grigorieva, I. V.; Firsov, A. A. Electric Field Effect in Atomically Thin Carbon Films. *Science* **2004**, *306*, 666–669.
2. Geim, A. K.; Novoselov, K. S. The Rise of Graphene. *Nat. Mater.* **2007**, *6*, 183–191.
3. Kopelevich, Y.; Esquinazi, P. Graphene Physics in Graphite. *Adv. Mater.* **2007**, *19*, 4559–4563.
4. Zhang, Y. B.; Tan, Y. W.; Stormer, H. L.; Kim, P. Experimental Observation of the Quantum Hall Effect and Berry's Phase in Graphene. *Nature* **2005**, *438*, 201–204.
5. Novoselov, K. S.; Geim, A. K.; Morozov, S. V.; Jiang, D.; Katsnelson, M. I.; Grigorieva, I. V.; Dubonos, S. V.; Firsov, A. A. Two-dimensional Gas of Massless Dirac Fermions in Graphene. *Nature* **2005**, *438*, 197–200.
6. Stankovich, S.; Dikin, D. A.; Dommett, G. H. B.; Kohlhaas, K. M.; Zimney, E. J.; Stach, E. A.; Piner, R. D.; Nguyen, S. T.; Ruoff, R. S. Graphene-Based Composite Materials. *Nature* **2006**, *442*, 282–286.
7. Ramanathan, T.; Abdala, A. A.; Stankovich, S.; Dikin, D. A.; Herrera-Alonso, M.; Piner, R. D.; Adamson, D. H.; Schniepp, H. C.; Chen, X.; Ruoff, R. S.; *et al*. Functionalized Graphene Sheets for Polymer Nanocomposites. *Nat. Nanotechnol.* **2008**, *3*, 327–331.
8. Wang, X.; Zhi, L. J.; Mullen, K. Transparent, Conductive Graphene Electrodes for Dye-Sensitized Solar Cells. *Nano Lett.* **2008**, *8*, 323–327.
9. Eda, G.; Fanchini, G.; Chhowalla, M. Large-Area Ultrathin Films of Reduced Graphene Oxide as a Transparent and Flexible Electronic Material. *Nat. Nanotechnol.* **2008**, *3*, 270–274.
10. Yoo, E.; Kim, J.; Hosono, E.; Zhou, H.; Kudo, T.; Honma, I. Large Reversible Li Storage of Graphene Nanosheet Families for Use in Rechargeable Lithium Ion Batteries. *Nano Lett.* **2008**, *8*, 2277–2282.
11. Vivekchand, S. R. C.; Rout, C. S.; Subrahmanyam, K. S.; Govindaraj, A.; Rao, C. N. R. Graphene-Based Electrochemical Supercapacitors. *J. Chem. Sci.* **2008**, *120*, 9–13.

12. Liu, Q.; Liu, Z. F.; Zhang, X. Y.; Zhang, N.; Yang, L. Y.; Yin, S. G.; Chen, Y. S. Organic Photovoltaic Cells Based on an Acceptor of Soluble Graphene. *Appl. Phys. Lett.* **2008**, *92*, 223303.
13. Wang, X.; Zhi, L. J.; Tsao, N.; Tomovic, Z.; Li, J. L.; Mullen, K. Transparent Carbon Films as Electrodes in Organic Solar Cells. *Angew. Chem., Int. Ed.* **2008**, *47*, 2990–2992.
14. Wu, Z. S.; Pei, S.; Ren, W.; Tang, D.; Gao, L.; Liu, B.; Li, F.; Liu, C.; Cheng, H. M. Field Emission of Single-Layer Graphene Films Prepared by Electrophoretic Deposition. *Adv. Mater.* 2008, DOI: 10.1002/adma200802560.
15. Mori, T.; Kikuzawa, Y.; Takeuchi, H. N-Type Field-Effect Transistor Based on a Fluorinated-Graphene. *Org. Electron.* **2008**, *9*, 328–332.
16. Schedin, F.; Geim, A. K.; Morozov, S. V.; Hill, E. W.; Blake, P.; Katsnelson, M. I.; Novoselov, K. S. Detection of Individual Gas Molecules Adsorbed on Graphene. *Nat. Mater.* **2007**, *6*, 652–655.
17. Berger, C.; Song, Z. M.; Li, X. B.; Wu, X. S.; Brown, N.; Naud, C.; Mayo, D.; Li, T. B.; Hass, J.; Marchenkov, A. N.; *et al.* Electronic Confinement and Coherence in Patterned Epitaxial Graphene. *Science* **2006**, *312*, 1191–1196.
18. Sutter, P. W.; Flege, J. I.; Sutter, E. A. Epitaxial Graphene on Ruthenium. *Nat. Mater.* **2008**, *7*, 406–411.
19. Stankovich, S.; Dikin, D. A.; Piner, R. D.; Kohlhaas, K. A.; Kleinhammes, A.; Jia, Y.; Wu, Y.; Nguyen, S. T.; Ruoff, R. S. Synthesis of Graphene-Based Nanosheets *via* Chemical Reduction of Exfoliated Graphite Oxide. *Carbon* **2007**, *45*, 1558–1565.
20. Stankovich, S.; Piner, R. D.; Nguyen, S. T.; Ruoff, R. S. Synthesis and Exfoliation of Isocyanate-Treated Graphene Oxide Nanoplatelets. *Carbon* **2006**, *44*, 3342–3347.
21. Li, D.; Muller, M. B.; Gilje, S.; Kaner, R. B.; Wallace, G. G. Processable Aqueous Dispersions of Graphene Nanosheets. *Nat. Nanotechnol.* **2008**, *3*, 101–105.
22. Gomez-Navarro, C.; Weitz, R. T.; Bittner, A. M.; Scolari, M.; Mews, A.; Burghard, M.; Kern, K. Electronic Transport Properties of Individual Chemically Reduced Graphene Oxide Sheets. *Nano Lett.* **2007**, *7*, 3499–3503.
23. Becerril, H. A.; Mao, J.; Liu, Z.; Stoltenberg, R. M.; Bao, Z.; Chen, Y. Evaluation of Solution-Processed Reduced Graphene Oxide Films as Transparent Conductors. *ACS Nano* **2008**, *2*, 463–470.
24. Hernandez, Y.; Nicolosi, V.; Lotya, M.; Blighe, F. M.; Sun, Z. Y.; De, S.; McGovern, I. T.; Holland, B.; Byrne, M.; Gun'ko, Y. K.; *et al.* High-Yield Production of Graphene by Liquid-Phase Exfoliation of Graphite. *Nat. Nanotechnol.* **2008**, *3*, 563–568.
25. Schniepp, H. C.; Li, J. L.; McAllister, M. J.; Sai, H.; Herrera-Alonso, M.; Adamson, D. H.; Prud'homme, R. K.; Car, R.; Saville, D. A.; Aksay, I. A. Functionalized Single Graphene Sheets Derived from Splitting Graphite Oxide. *J. Phys. Chem. B* **2006**, *110*, 8535–8539.
26. McAllister, M. J.; LiO, J. L.; Adamson, D. H.; Schniepp, H. C.; Abdala, A. A.; Liu, J.; Herrera-Alonso, M.; Milius, D. L.; CarO, R.; Prud'homme, R. K.; *et al.* Single Sheet Functionalized Graphene by Oxidation and Thermal Expansion of Graphite. *Chem. Mater.* **2007**, *19*, 4396–4404.
27. Wu, Z. S.; Ren, W.; Gao, L.; Liu, B.; Jiang, C.; Cheng, H. M. Synthesis of High-Quality Graphene with a Predetermined Number of Layers. *Carbon* **2009**, *47*, 493–499.
28. Li, X. L.; Zhang, G. Y.; Bai, X. D.; Sun, X. M.; Wang, X. R.; Wang, E.; Dai, H. J. Highly Conducting Graphene Sheets and Langmuir−Blodgett Films. *Nat. Nanotechnol.* **2008**, *3*, 538–542.
29. Kratschmer, W.; Lamb, L. D.; Fostiropoulos, K.; Huffman, D. R. Solid C_{60}: A New Form of Carbon. *Nature* **1990**, *347*, 354–358.
30. Zhao, X.; Ohkohchi, M.; Wang, M.; Iijima, S.; Ichihashi, T.; Ando, Y. Preparation of High-Grade Carbon Nanotubes by Hydrogen Arc Discharge. *Carbon* **1997**, *35*, 775–781.
31. Iijima, S.; Ichihashi, T. Single-Shell Carbon Nanotubes of 1-nm Diameter. *Nature* **1993**, *363*, 603–605.
32. Liu, C.; Cong, H. T.; Li, F.; Tan, P. H.; Cheng, H. M.; Lu, K.; Zhou, B. L. Semicontinuous Synthesis of Single-Walled Carbon Nanotubes by a Hydrogen Arc Discharge Method. *Carbon* **1999**, *37*, 1865–1868.
33. Liu, Q. F.; Ren, W. C.; Li, F.; Cong, H. T.; Cheng, H. M. Synthesis and High Thermal Stability of Double-Walled Carbon Nanotubes Using Nickel Formate Dihydrate as Catalyst Precursor. *J. Phys. Chem. C* **2007**, *111*, 5006–5013.
34. Huang, H. J.; Kajiura, H.; Tsutsui, S.; Murakami, Y.; Ata, M. High-Quality Double-Walled Carbon Nanotube Super Bundles Grown in a Hydrogen-Free Atmosphere. *J. Phys. Chem. B* **2003**, *107*, 8794–8798.
35. Hummers, W.; Offman, R. Preparation of Graphitic Oxide. *J. Am. Chem. Soc.* **1958**, *80*, 1339.
36. Falcao, E. H. L.; Blair, R. G.; Mack, J. J.; Viculis, L. M.; Kwon, C. W.; Bendikov, M.; Kaner, R. B.; Dunn, B. S.; Wudl, F. Microwave Exfoliation of a Graphite Intercalation Compound. *Carbon* **2007**, *45*, 1367–1369.
37. Verdejo, R.; Barroso-Bujans, F.; Rodriguez-Perez, M. A.; de Saja, J. A.; Lopez-Manchado, M. A. Functionalized Graphene Sheet Filled Silicone Foam Nanocomposites. *J. Mater. Chem.* **2008**, *18*, 2221–2226.
38. Ferrari, A. C. Raman Spectroscopy of Graphene and Graphite: Disorder, Electron-Phonon Coupling, Doping and Nonadiabatic Effects. *Solid State Commun.* **2007**, *143*, 47–57.
39. Ferrari, A. C.; Meyer, J. C.; Scardaci, V.; Casiraghi, C.; Lazzeri, M.; Mauri, F.; Piscanec, S.; Jiang, D.; Novoselov, K. S.; Roth, S.; *et al.* Raman Spectrum of Graphene and Graphene Layers. *Phys. Rev. Lett.* **2006**, *97*, 187401.
40. Kudin, K. N.; Ozbas, B.; Schniepp, H. C.; Prud'homme, R. K.; Aksay, I. A.; Car, R. Raman Spectra of Graphite Oxide and Functionalized Graphene Sheets. *Nano Lett.* **2008**, *8*, 36–41.
41. Ferrari, A. C.; Robertson, J. Interpretation of Raman Spectra of Disordered and Amorphous Carbon. *Phys. Rev. B* **2000**, *61*, 14095–14107.
42. Pimenta, M. A.; Dresselhaus, G.; Dresselhaus, M. S.; Cançado, L. G.; Jorio, A.; Saito, R. Studying Disorder in Graphite-Based Systems by Raman Spectroscopy. *Phys. Chem. Chem. Phys.* **2007**, *9*, 1276–1291.
43. Sato, K.; Saito, R.; Oyama, Y.; Jiang, J.; Cançado, L. G.; Pimenta, M. A.; Jorio, A.; Samsonidze, G. G.; Dresselhaus, G.; Dresselhaus, M. S. D-band Raman Intensity of Graphitic Materials as a Function of Laser Energy and Crystallite Size. *Chem. Phys. Lett.* **2006**, *427*, 117–121.
44. Hutchison, J. L.; Kiselev, N. A.; Krinichnaya, E. P.; Krestinin, A. V.; Loutfy, R. O.; Morawsky, A. P.; Muradyan, V. E.; Obraztsova, E. D.; Sloan, J.; Terekhov, S. V.; *et al.* Double-Walled Carbon Nanotubes Fabricated by a Hydrogen Arc Discharge Method. *Carbon* **2001**, *39*, 761–770.
45. Takai, K.; Oga, M.; Sato, H.; Enoki, T.; Ohki, Y.; Taomoto, A.; Suenaga, K.; Iijima, S. Structure and Electronic Properties of a Nongraphitic Disordered Carbon System and Its Heat-treatment Effects. *Phys. Rev. B* **2003**, *67*, 214202–214212.
46. Ding, F.; Jiao, K.; Wu, M.; Yakobson, B. I. Pseudoclimb and Dislocation Dynamics in Superplastic Nanotubes. *Phys. Rev. Lett.* **2007**, *98*, 075503.
47. Ding, F.; Jiao, K.; Lin, Y.; Yakobson, B. I. How Evaporating Carbon Nanotubes Retain Their Perfection. *Nano Lett.* **2007**, *7*, 681–684.
48. Zhang, Z. Y.; Yao, K.; Liu, Y.; Jin, C. H.; Liang, X. L.; Chen, Q.; Peng, L. M. Quantitative Analysis of Current−Voltage Characteristics of Semiconducting Nanowires: Decoupling of Contact Effects. *Adv. Funct. Mater.* **2007**, *17*, 2478–2489.